UCTEA Chamber of Geophysical Engineers of TURKEY
Society of Exploration Geophysicists
INTERNATIONAL GEOPHYSICAL CONFERENCE AND OIL & GAS EXHIBITION
ISTANBUL 2012

Multisource Full Waveform Inversion with Topography Using Ghost Extrapolation

Dongliang Zhang, Ge Zhan and Wei Dai, King Abdullah University of Science and Technology*

Summary

Standard finite-difference modeling of the wave equation for models with severe topographic changes in elevation generates artificial diffractions in the synthetic traces. This can lead to unacceptable inaccuracies in the velocity tomogram computed by full waveform inversion (FWI). To alleviate this problem we propose a polynomial interpolation of the field values at and near the irregular free surface. This improved finite-difference procedure is denoted as the ghost extrapolation method. To validate its effectiveness, synthetic data are computed from a Marmousi model with severe topographical variations of the free surface. These data are inverted using both the standard FWI and the phase-encoded multisource FWI methods. Results show the ghost extrapolation method is effective in eliminating noticeable artifacts and producing accurate tomograms.

Introduction

Standard finite-difference modeling of the wave equation for models with severe topographic changes in elevation generates artificial diffractions in the synthetic traces. This can lead to unacceptable inaccuracies in the velocity tomogram computed by full waveform inversion (FWI). To alleviate this problem we propose a polynomial interpolation of the field values at and near the irregular free surface. This improved finite-difference procedure is denoted as the ghost extrapolation method. To validate its effectiveness, synthetic data are computed from a Marmousi model with severe topographical variations of the free surface. These data are inverted using both the standard FWI and the phase-encoded multisource FWI methods. Results show the ghost extrapolation method is effective in eliminating noticeable artifacts and producing accurate tomograms.

The primary methods for forward modeling with topography mainly include the boundary element (Perrey-Debain et al., 2004; Carrer and Mansur, 2010), finite element (Ke et al., 2001) and finite difference methods. Among them, the boundary element and finite element methods are most adaptable to irregular surfaces. However, the boundary element method is restricted to simple models and the finite element often requires an excessive increase in computation time. In addition, the finite element method must generate a complicated mesh grid, whose quality will affect the accuracy of the solution.

The most common modeling method in seismic exploration is the finite difference method, but it cannot easily accommodate free surfaces with irregular topography unless the grid spacing is very fine. A simple approach is to apply the vacuum method (Graves, 1996), which sets the elastic parameters to zero at and above the free surface (or a very low velocity). However, due to the staircase approximation to the topography, it is easy to generate diffractions unless there is a very fine grid spacing. Levander (1988) first proposed the fourth-order accurate image method in the flat surface case, then Robertsson (1996) developed and applied the image method to the irregular surface. Just like the vacuum method, the image method also adopts the staircase approximation; therefore, the diffraction problem still exists. In addition, a coordinate transform or a curvilinear grid method (Hestholm and Ruud, 1998; Zhang and Chen, 2006) can be adopted as well, and the former is a special case of the latter. That is, the curvilinear grid in the physical space is transformed into the regular grid in the computing space, which involves a coordinate transformation or curvilinear grid generation. In addition, the wave equation needs to be modified according to a more complex wave equation.

In order to avoid the drawbacks of the above methods, we introduce the ghost method from fluid mechanics (Frederic and Ronald, 2005) and use the virtual extrapolation technique in the Cartesian grid. This new approach avoids the generation of diffractions associated with the staircase approximation of topography and eliminates artificial diffraction. Our approach will allow for an accurate application of FWI to seismic data collected on surfaces with strong elevation changes. This claim is validated by our tests on the data generated from the Marmousi model with irregular topography.

Ghost extrapolation

The acoustic wave equation

$$\frac{\partial^2 P}{\partial x^2}+\frac{\partial^2 P}{\partial z^2}=\frac{1}{v^2}\frac{\partial^2 P}{\partial t^2}, \qquad (1)$$

for a model with a free surface boundary condition means that the pressure is zero on the surface, where P is the pressure and v is the velocity. The fourth-order finite-difference scheme requires the center point to have two

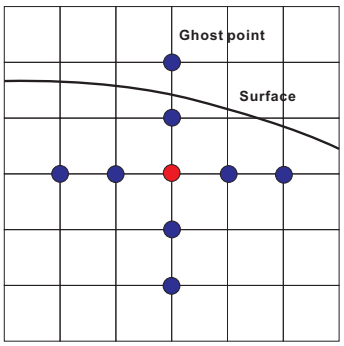

Figure 1: The fourth-order scheme, where the center point is near the surface and some points of the FD stencil extend above the free surface; these extended points are called ghost points.

points along each of the four directions shown in Figure 1. When the center point is close to the surface, some of these points extend above the free surface, and we call these points the ghost points (see Figure 1). Considering the z direction (see Figure 2a), so the differencing scheme can be written as

$$\frac{\partial^2 P}{\partial z^2} = -\frac{1}{12}P_{i-2,j} + \frac{4}{3}P_{i-1,j} - \frac{5}{2}P_{i,j} + \frac{4}{3}P_{i+1,j} - \frac{1}{12}P^G_{i+2,j}, \quad (2)$$

Where i, j are the node indices and the superscript G indicates this point is the ghost point. The key issue is how to get the value of ghost point in order to calculate the second-order derivative of the pressure at this point. Physically the pressure of the ghost point in the air should be zero. In this case, the virtual value of the ghost point can be estimated by using a polynomial extrapolation method. Towards this goal, assume that the wave field near the surface is a local cubic function

$$\tilde{P}(z) = az^3 + bz^2 + cz + d, \quad (3)$$

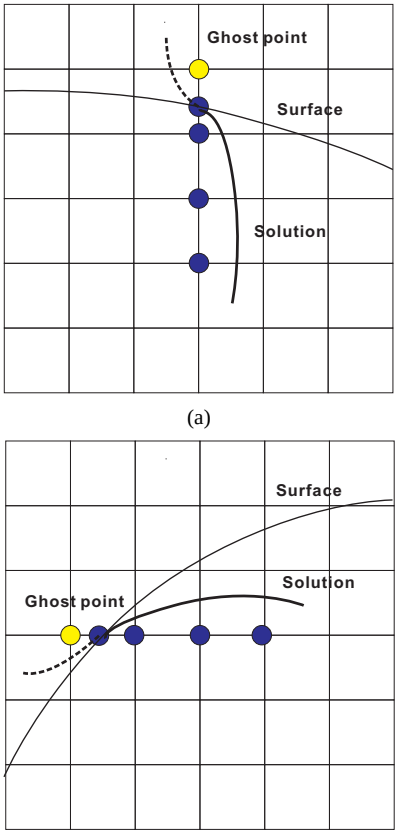

Figure 2: Ghost extrapolation. a) Ghost extrapolation in the z direction. We assume the solution near the surface is a local cubic function, then choose four blue points to calculate the coefficients of the cubic function; then extrapolate the pressure to the yellow point. b) The ghost extrapolation in the x direction is the same as that for the z direction.

Where a, b, c and d are the coefficients, and then select the four points to calculate these coefficients. It is extremely important that the selected four points contain a point on the free boundary to satisfy the boundary condition. The second step is to extrapolate the pressure on the ghost point utilizing a cubic interpolation polynomial. With the ghost point values, the second-order derivative in the z direction of the points near the surface can be calculated. Process the same procedure for the x (Figure 2b) and z directions, where the x and z directions are independent in this method, so that for some ghost points, both the extrapolation values in x and z direction should be calculated. A modified improvement of this method is to perform the extrapolation using a two- or three-dimensional polynomial, but we will restrict our tests to the one-dimensional interpolation.

The ghost extrapolation does not require an approximation to the surface topography, so it will not generate diffractions for those when the standard finite difference method is used. As an example, Figure 3 shows a simple two-layer inclined surface model and Figure 4a shows the common shot gather computed by a FD scheme with the ghost point extrapolation method. In comparison, Figure 4b depicts the common shot gather computed by a FD method with the commonly used image boundary condition, and obvious diffractions can be seen. Finally, Figure 4c shows the common shot gather computed by a FD method with a vacuum free-surface condition, and obvious diffractions also can be seen.

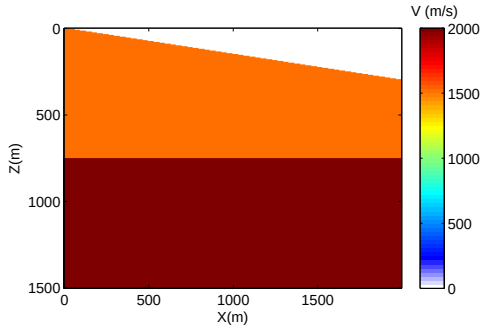

Figure 3: Two layer dipping surface model.

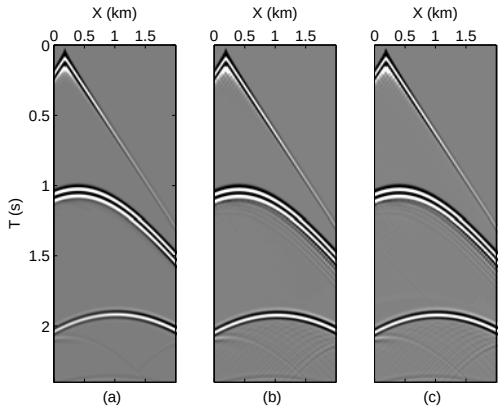

Figure 4: Common shot gathers computed by different FD modeling methods. a) Using the ghost extrapolation method, where there are no diffractions. The CSGs computed by FD methods that use b). image boundary conditions and c). vacuum boundary conditions show obvious diffractions.

Full waveform inversion test on Marmousi model

The traditional Marmousi model has been modified by adding an irregular surface with peaks and valleys. The model size is 301×400 with a grid spacing of 5 m. There

are 200 shots and 400 receivers with the 20 Hz Ricker wavelet. Figure 5 is the true velocity model and Figure 6 shows a single shot gather generated from the true velocity model. Figure 7 is the initial velocity model after the application of a smoothing filter. Figure 8 shows the results after 85 iterations of an iterative FWI method that uses a conjugate gradient method. Compared with the true velocity model, it can be found that the shallow and deep parts of the tomogram have relatively high resolution.

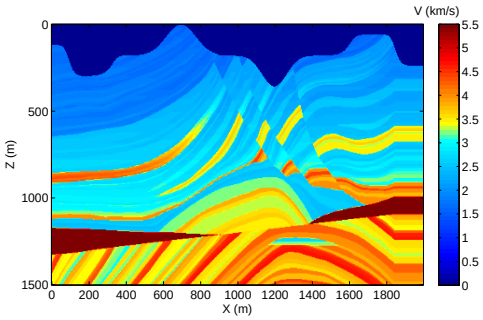

Figure 5: The true Marmousi velocity model with topography.

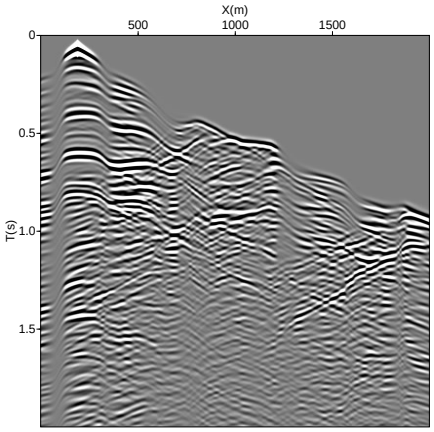

Figure 6: Synthetic common shot gather associated with the Marmousi model.

In order to reduce the CPU time of FWI, we apply phase-encoding (Romero et al., 2000; Krebs et al., 2009; Zhan et al., 2010; Dai et al., 2011) of shot records to simultaneously migrate a number of shot gathers within a single iteration. Figure 9 is the result of multisource FWI after 85 iterations, where we combine 200 phase-encoded CSGs. Choosing three positions x=400 m, x=1000 m and x=1500 m, the comparison of the true velocity and the inverted results for single source and multi-source FWI velocity profiles in the vertical direction is shown in Figure 10. Figure 11 is the plot of iteration number versus waveform residual for single source and multi-source FWI, and shows rapid convergence to a small misfit value.

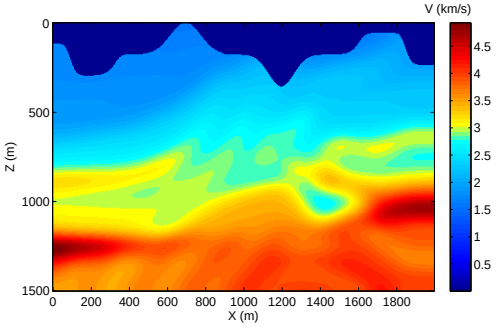

Figure 7: Initial velocity model for full waveform inversion.

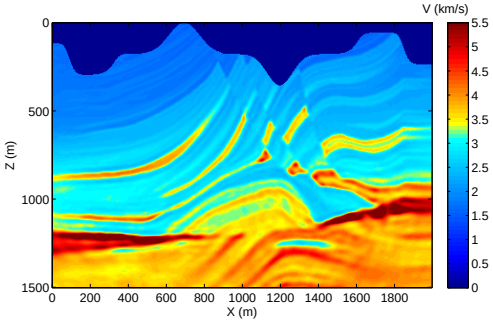

Figure 8: Full waveform inversion result after 85 iterations.

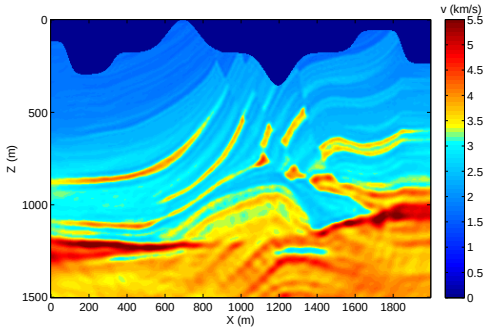

Figure 9: Waveform inversion result using multi-source shot gathers.

Conclusions

We propose the ghost extrapolation method for estimating the values of the pressure field near free surfaces with irregular topography. Numerical modeling results show no artificial diffractions generated by the stair-step boundary compared to the artifacts generated by the standard FD method. Results also show that this method is effective for standard FWI and phase-encoded multisource FWI applied to Marmousi data with irregular topography. The next step is to test this method on elastic data.

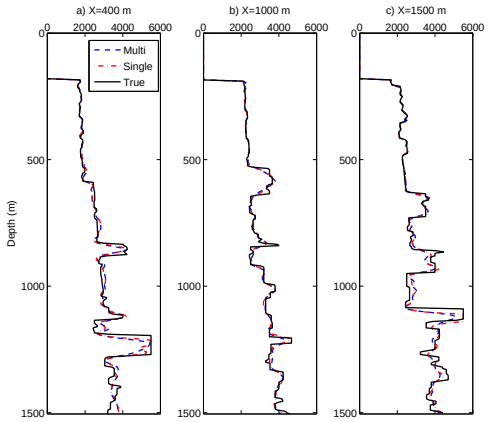

Figure 10: Comparison of true velocity and inverted results of single source and multi-source in the vertical direction at different locations.

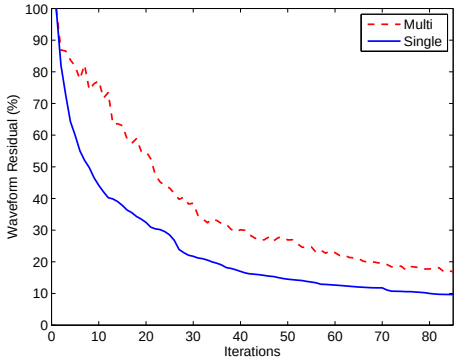

Figure 11: The normalized wavefom residuals versus iterations.

Acknowledgments

We are grateful to the sponsors of the Center for Subsurface Imaging and Fluid Modeling (CSIM). The first author would like to thank KAUST for providing me the postdoctoral fellowship.

References

Boonyasiriwat, C., G. T. Schuster, P. Valasek, and W. Cao, 2010, Applications of multiscale waveform inversion to marine data using a flooding technique and dynamic early-arrival windows: Geophysics,75, R129–R136.

Bunks, C., F. M. Saleck, S. Zaleski, and G. Chavent, 1995, Multiscale seismic waveform inversion: Geophysics, 60, 1457–1473.

Carrer, J. A. M., and W. J. Mansur, 2010, Scalar wave equation by the boundary element method: A d-bem approach with constant time-weighting functions: International Jour-nal for Numerical Methods in Engineering, 81, 1281–1291.

Charles, S., and R. G. Pratt, 2008, Frequency-domain waveform tomography in the foothills: Velocity model estimation with synthetic long-offset data: CSPG CSEG CWLS Convention, 394–398.

Dai, W., X. Wang, and G. T. Schuster, 2011, Least-squares migration of multisource data with a deblurring filter: Geophysics,76, R135–R146.

Frederic, G., and F. Ronald, 2005, A fourth order accurate discretization for the laplace and heat equations on arbitrary domains, with applications to the stefan problem: Journal of Computational Physics,22, 577601.

Graves, R., 1996, Simulating seismic wave propagation in 3d elastic media using staggered-grid finite difference: Bulletin on the Seismological Society of Ameria, 86, 1091– 1106.

Hestholm, S., and B. Ruud, 1998, 3d finite-difference elastic wave modeling including surface topography: Geophysics, 63, 613–622.

Ke, B., B. Zhao, J. Cai, and Z. Tian, 2001, 2d finite element acoustic wave modeling including rugged topography: SEG Technical Program Expanded Abstracts, 1199–1202.

Krebs, J. R., J. E. Anderson, D. Hinkley, R. Neelamani, S. Lee, A. Baumstein, and M.D. Lacasse, 2009, Fast full-wavefield seismic inversion using encoded sources: Geophysics, 74, WCC177–WCC188.

Levander, A. R., 1988, Fourth-order finite-difference p-sv seismograms: Geophysics, 53, 1425–1436.

Luo, Y., and G. T. Schuster, 1991, Wave-equation traveltime inversion: Geophysics, 56, 645–653.

Nemeth, T., E. Normark, and F. Qin, 1997, Dynamic smoothing in crosswell traveltime tomography: Geophysics, 62, 168–176.

Perrey-Debain, E., J. Trevelyan, and P. Bettess, 2004, Wave boundary elements: a theoretical overview presenting applications in scattering of short waves: Engineering Analysis with Boundary Elements, 28, 131–141.

Pratt, R. G., 1999, Seismic waveform inversion in the frequency domain, part 1: Theory and verification in a physical scale model: Geophysics, 64, 888–901.

Robertsson, J. O. A., 1996, A numerical free-surface condition for elastic/viscoelastic finite-difference modelingin the presence of topography: Geophysics, 61, 1921–1934.

Romero, L. A., D. C. Ghiglia, C. C. Ober, and S. A. Morton, 2000, Phase encoding of shot records in prestack migration: Geophysics, 65, 426–436.

Sava, P., and I. Vlad, 2008, Numeric implementation of wave-equation migration velocity analysis operators: Geophysics, 73, VE145–VE159.

Sirgue, L., and R. G. Pratt, 2004, Efficient waveform inversion and imaging: A strategy for selecting temporal frequencies: Geophysics, 69, 231–248.

Zhan, G., W. Dai, C. Boonyasiriwat, and G. T. Schuster, 2010, Acoustic multi-source waveform inversion with deblurring: EAGE Expanded Abstracts, G002.

Zhang, W., and X. Chen, 2006, Traction image method for irregular free surface boundaries in finite difference seismic wave simulation: Geophysical Journal International, 167, 337–353.

Zhang, W., and J. Zhang, 2011, Full waveform tomography with consideration for large topography variations: SEG Technical Program Expanded Abstracts, 2539–2542